Effect of Water on the Molecular Mobility of Elastin

Valerie Samouillan,* Cédric André, Jany Dandurand, and Colette Lacabanne

Laboratoire de Physique des Polymères, CIRIMAT UMR 5085, Université Paul Sabatier, 31062 Toulouse Cedex 4, France

Received October 29, 2003; Revised Manuscript Received January 16, 2004

Purified and hydrated elastin is studied by both thermal and dielectric techniques to have insight into the chain dynamics of this protein. By differential scanning calorimetry, the glassy behavior of elastin is highlighted; the glass transition temperature (T_g) of elastin is found to be widely dependent on hydration, falling from 200 °C in the dehydrated state to 30 °C for 30% hydration. A limit of T_g at around 0 °C is found when crystallizable water is present in the system, that is, when the formation of ice prevents motions of some 10 nm along the polypeptidic chains. The technique of thermally stimulated currents, carried out in the −180 to 0 °C temperature range, is useful to detect localized motions. In this case, too, the localized motions vary considerably according to hydration: a first relaxation mode is observed at −145 °C and it is associated with the reorientation of crystallizable water in ice *I*; a second relaxation mode, more complex and cooperative, occurs at around −80 °C and could be attributed to the complex constituted by the dipolar groups of the polypeptidic chain and noncrystallizable water, behaving as a glassy system.

Introduction

The main property of elastin, one of the major proteins of connective tissues, is to impart elasticity to organs and tissues, even if this protein not only is considered at present as a simple structural material but also plays a role in several biological mechanisms.[1]

Mature elastin is an insoluble network obtained after the reticulation of tropoelastine molecules in the extracellular space, according to a complex process involving the alignment of monomers by microfibrils, deamination, and oxidation of lysyl residues into allysine, which reacts to form the specific cross-links of elastin.[2,3]

The remarkable properties of hydrated elastin have aroused several studies to elucidate the structure−function relationship of this natural elastomer. This knowledge would be very important to understand the pathologies of elastic fibers and to conceive new biomaterials with interesting elastic properties.[4] Several models, which largely differ according to the analyzed data (microscopy,[5] molecular simulation,[1] thermal and mechanical properties,[6,7] etc.) were established. First, experimental results on elastin led to a controversy: on one hand, elastin was considered as a random network, acting like an amorphous synthetic elastomer, with an elasticity of entropic origin;[6] on the other hand, the presence of defined structures at the molecular level were evidenced (α helices in the polyalanine zones,[8] β turns in sequences containing the X−P−G structural unit)[9−11] and led to anisotropic models for elastin.[9,12] Different recurring sequences of elastin were then carefully analyzed through the synthesis of analogous polypeptides or, more recently, through molecular dynamics simulation, resulting in different models: Urry et al.'s model[13] on VPGVG sequences that form β spirals, which deals with a librational entropy that varies between the stretched and extended states, providing the force for return to the relaxed state.[13] Debelle and Tamburro's model[1] proposed for the GXGGX sequences brings to the forefront isolated and labile β turns, resulting in a fluctuant polypeptidic chain, with chaotic motions, in the relaxed state. The dynamic entropy of the system significantly decreases in the stretched and more structured state, and the classical theory of rubber elasticity can so be applied to these sequences. According to Li and Daggett,[14] elastin can be described as a two-phase model consisting of hydrophilic cross-linking domains rich in lysine and alanine and dynamic hydrophobic domains responsible for elasticity. The hydrophobic domains would be best described as a compact amorphous structure with distorted P strands, fluctuating turns, buried hydrophobic residues, and main-chain polar atoms forming hydrogen bonds with water. The determinant role of water must not be forgotten in the phenomenon of elasticity because water makes elastin extremely dynamic in its relaxed state.[1,14]

As a result of its numerous cross-links and its hydrophobic nature, elastin constitutes a very insoluble network and cannot be analyzed by the usual techniques of characterization of proteins. In a previous work,[15] we have studied the chain dynamics of elastin in the dehydrated state to evidence the intrinsic motions of this biopolymer. Nevertheless, in the physiological conditions, elastin is solicited in the hydrated state (around 40−50% of hydration). So it is necessary to follow the evolution of the chain dynamics with hydration and to compare it with the results obtained in the dehydrated state, to evaluate the determinant role of water. For this purpose, we propose the use of differential scanning calorimetry (DSC), which gives information on the physical structure of elastin with temperature, and the thermostimulated currents technique, which allows scanning motions at the nanometer scale.

* Corresponding author: Laboratoire de Physique des Polymères, Bat 3R1B2, 118, Route de Narbonne − Université Paul Sabatier, 31062 Toulouse Cedex 04, France. E-mail: vsamou@cict.fr.

10.1021/bm034436t CCC: $27.50
Published on Web 04/21/2004

Experimental Section

1. Materials. Insoluble elastin was purified from bovine ligament neck by Lansing et al.'s method[16] and was freeze-dried. Samples of different hydration levels have been studied. The 0% hydration has been obtained by drying samples above P_2O_5 at 105 °C during 12 h. Other samples were equilibrated to constant humidity by storage at 25 °C over saturated salt solutions during 24 h and then submitted to different vacuum periods in the cell measurement, at controlled temperatures. For high hydration levels, samples were directly immersed in distilled water and then carefully dried on appropriate paper to eliminate the excess of water.

In all the cases, the water content of the samples was determined from the loss of weight after drying to constant weight above P_2O_5 at 105 °C. The hydration level, h(%), is defined as follows:

$$h(\%) = \frac{m_{\text{water}}}{m_{\text{elastin}}} \times 100$$

where m_{water} is the mass of water and m_{elastin} is the mass of elastin.

In this study, hydration levels of samples vary between 0 and 60%.

2. DSC. The DSC thermograms were recorded with a TA Instrument DSC 2920 differential scanning calorimeter. Samples (2−5 mg) were sealed into hermetic aluminum pans, and empty pans were used as references. Investigations were performed in the −30 to +250 °C zone with a 5 °C/min heating rate. The order temperature can be written as follows:

$$T = T_0 + qt$$

where T_0 is the initial temperature, q is the heating rate, and t is the time.

3. Modulated Differential Scanning Calorimetry (MDSC). The same apparatus was used for this analysis. In this case, a sinusoidal component is added to the linear heating rate, and the order temperature can be written as follows:

$$T = T_0 + qt + A_q \sin[(2\pi/z)t]$$

where A_q is the amplitude of modulation, z is the period of modulation, and t is the time. In our experiments, $A_q = 1$ °C and $z = 60$ s.

This temperature modulation allows a modulated heat flow to be recorded, which can be decomposed by Fourier's analysis in two distinct heat flows, the former in phase with the temperature (reversing heat flow) and the latter out of phase with the temperature[17] (nonreversing heat flow).

4. Thermally Stimulated Currents (TSC). *4.1. Global TSC Spectra.* TSC measurements were carried out with a setup developed in our laboratory and previously described.[18] Samples were placed between two plate stainless steel electrodes, and the sample cell was flushed and filled with dry He. The TSC relaxation spectra were recorded with a very sensitive electrometer (Keithley 642, 10^{-16} A accuracy) versus temperature during a linear heating rate (7 °C/min, which represents an ideal compromise between signal resolution and temperature regulation) after a static polarization at a given temperature and freezing at liquid nitrogen temperature. In the present study, the best polarization conditions resulting in reproducible dipolar relaxations were as follows: polarization field $E_p = 400$ V/mm, polarization time $t_p = 2$ min, linear heating rate $q = 7$ °C/min.

4.2. Fractional Polarizations (FP). In polymers, the TSC peaks corresponding to dipolar relaxations are in general too broad to be associated with only one single relaxation process, that is, with only one relaxation time. In fact, these broad peaks correspond to a distribution of relaxation times involved in the same dipolar mechanism. The FP procedure can be used to decompose a complex TSC peak in elementary processes that contribute to a complex dielectric relaxation. In this procedure, each isolated spectrum is well approximated by a single relaxation time, allowing Bucci et al.'s analysis.[19] In the FP procedure, the electric field E_p is applied at T_p for 2 min, allowing the orientation of dipoles with relaxation time $\tau(T_p)$ lower than 2 min. The temperature is then lowered by ΔT to T_d ($\Delta T = 5$ °C) under field. At T_d, the field is turned off and the sample is then held for 2 min so that dipoles with relaxation time $\tau(T_d)$ lower than 2 min relax. The sample is then quenched to $T_0 \ll T_d$ so that only dipoles with relaxation time $\tau(T)$ such as $\tau(T_p) < 2$ min and $\tau(T_d) > 2$ min remain oriented at T_0. The depolarization current is recorded in a similar fashion as just mentioned for the complex spectrum. The response of this FP experiment is the result of the reorientation of a narrow distribution of relaxation times excited over a $\Delta T = 5$ °C temperature window around T_p. By increasing the value of T_p by steps of 2.5 °C along the temperature axis, the whole TSC spectrum is resolved into a series of fractional depolarization peaks, allowing us to reach experimentally the distribution of the global dipolar relaxation.

In Bucci et al.'s framework based on the classical Debye treatment with a single relaxation time τ, the decay of the polarization $P(t)$ after removal of the static field is given by

$$P(t) = P_0 \exp(-t/\tau)$$

where P_0 is the saturation polarization. The corresponding depolarization current density at time t is given by

$$J(t) = -\mathrm{d}P(t)/\mathrm{d}t = P(t)/\tau$$

As the decay of the frozen-in polarization is thermally stimulated, time and temperature are related by a linear relationship, $T = T_0 + qt$, where q is the heating rate. The relaxation time τ is also temperature dependent and can be written as

$$\tau(T) = P(T)/J(T) \quad \text{with} \quad P(T) = q^{-1}\int_T^{T_f} J(T')\,\mathrm{d}T'$$

Therefore, the temperature dependence of the relaxation time for an elementary peak can be deduced from the ratio between $I(T)$ and the remaining area under the peak from T to T_f, the temperature at which the depolarization current returns to zero.

Results and Discussion

1. Thermal Transitions. Figure 1 corresponds to the MDSC thermogram of freeze-dried elastin; as shown in

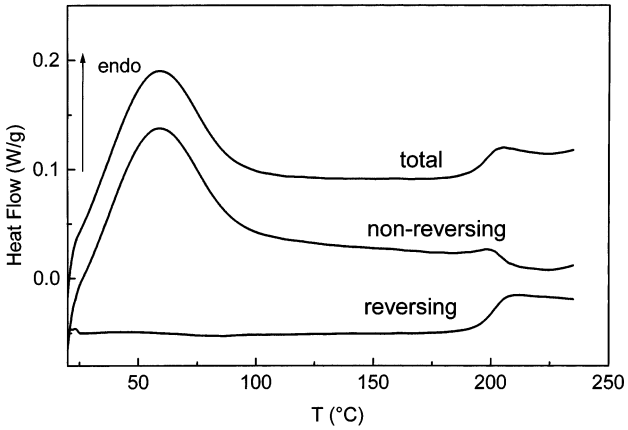

Figure 1. MDSC thermogram of freeze-dried elastin.

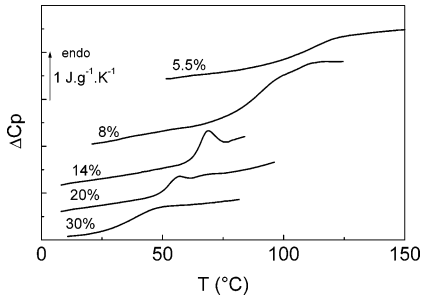

Figure 2. DSC thermograms of differently hydrated elastins. The hydration level *h* is given for each thermogram.

previous works,[1] the total heat flow, which corresponds to the classical heat flow recorded in DSC experiments, presents two main thermal events: an endothermic peak at around 80 °C, associated with the loss of noncrystallizable water with temperature, and a more complex event at 200 °C, corresponding to the glass transition T_g (i.e., the transition from a glassy to a rubbery state) of dehydrated elastin. Analysis of the reversing and nonreversing heat flows allows us to point out these different events; as a matter of fact, pseudo-second-order transitions such as glass transitions are known to be present on the reversing heat flow and endothermic phenomena (like fusion, vaporization, etc.) on the nonreversing heat flow.[17] On the reversing heat flow, only the jump of the specific heat corresponding to the glass transition is observed, whereas the nonreversing heat flow signal presents the extrinsic transition due to the water loss at 80 °C and a weak endothermic peak at around 200 °C, assigned to the structural relaxation of elastin (i.e., the disruptions of hydrogen bonds between N—H and C═O groups of the polypeptidic chain, formed during the physical aging[21] of elastin at a temperature below T_g).

The thermal glass transition of elastin can be directly connected to its mechanical properties because the T_g zone corresponds to a viscoelastic state of the biopolymer.[20] That is the reason we chose to follow the evolution of T_g with hydration.

On Figure 2, the thermograms of differently hydrated elastins, from 5.5 to 30% hydration levels, are superimposed. In this case, these results arise from DSC experiments because the sealed pans used to maintain a constant hydration are too massive for fitting the exact modulated temperature. Only the interesting zone of each thermogram, where the glass transition occurs, is presented.

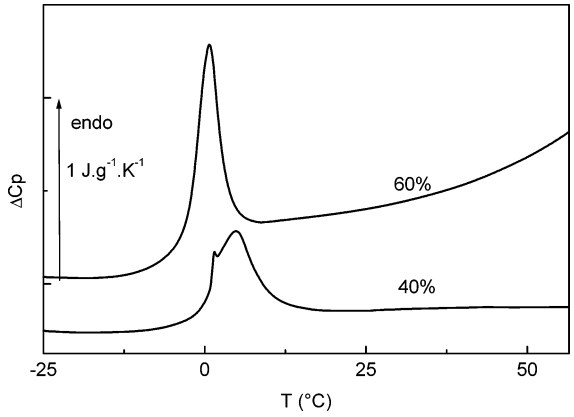

Figure 3. DSC thermograms of highly hydrated elastins. The hydration level *h* is given for each thermogram.

As we can see, the step of the specific heat is widely dependent on hydration: a hydration of 5.5% makes T_g decrease from 200 to 100 °C, and a hydration of 30% brings T_g to the ambient temperature. As previously observed for several polymer/solvent systems,[20] water has a strong plasticizing effect on elastin: on a mechanical point of view, the drastic fall of T_g with hydration means that the viscoelastic properties of elastin are closely connected to the water content of fibers. These results confirm the essential role of water in the molecular dynamics of elastin as predicted by Tamburro et al.'s model:[1,22−24] undoubtedly, water facilitates the motions of the polypeptide chains, and the hydrated relaxed protein must undergo mainly chaotic, Brownian-like motions, behaving as a fractal system of high entropy.[22,24]

Moreover, we can observe a nonnegligible structural relaxation on the thermograms of 14 and 20% hydrated elastins: these endothermic peaks correspond to a physical aging, a reversible phenomenon that can be erased by thermal cycling. These relaxation phenomena are connected to the storage time of the samples at around $T_g = 20$ °C and $T_g = 30$ °C: the longer this time is, the more important is the structural rearrangement.[21] In the case of the 14 and 20% hydrated samples, equilibrated at 25 °C over salt solutions during 24 h, the ideal conditions are right for an important physical aging. Complementary studies[25] were performed on the same sample of hydrated elastin, submitted to different thermal cycling, to confirm this physical aging. On the contrary, the 8% hydrated sample cannot undergo a large physical aging at 25 °C because its glass transition temperature is higher, and 24 h of storage is not sufficient to detect a structural arrangement. As for the 30% hydrated sample, it was prepared by immersion in water just before the experiment and so does not undergo physical aging.

This calorimetric study was carried out for high hydration levels; the thermograms corresponding to 40 and 60% hydration levels are presented in Figure 3.

In this case, an endothermic peak, which does not disappear with thermal cycling, is superimposed to the step of the specific heat. In accordance with previous works on different polymer/water systems,[26−29] this peak is associated with the melting of bulk water. It corresponds to the crystallizable water contained in the system. This kind of water is present for a hydration level higher than 30%.

The glass transition temperature was computed from all the thermograms, and we have reported in Figure 4 the

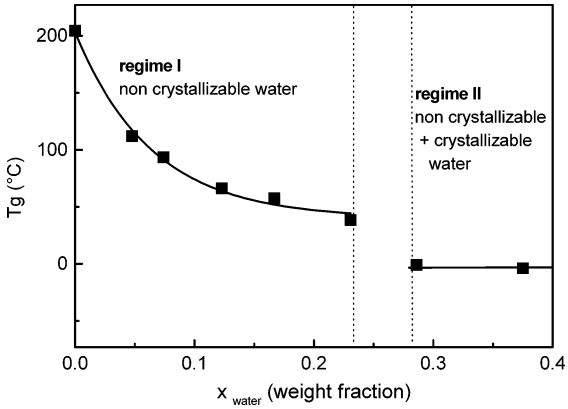

Figure 4. Evolution of the glass transition temperature of elastin with the weight fraction of water.

variation of T_g with the weight fraction of water, defined as follows:

$$x_{water} = \frac{m_{water}}{m_{water} + m_{elastin}} = \frac{h}{h + 100}$$

where m_{water} is the mass of water, $m_{elastin}$ is the mass of elastin, and h is the hydration level in percent.

Figure 3 clearly shows two regimes of hydration for elastin. In regime I, that is, for a water weight fraction inferior to $x = 0.2$, corresponding to noncrystallizable water, the glass transition temperature of elastin varies according to the Fox−Flory law, for which a hydrated polymer is considered as a monophased blend:

$$\frac{1}{T_g} = \frac{1 - x_{water}}{T_{g,elastin}} + \frac{x_{water}}{T_{g,water}}$$

where T_g is the glass transition of hydrated elastin, $T_{g,elastin}$ is the glass transition of dehydrated elastin (200 °C), $T_{g,water}$ is the glass transition of quenched pure water (estimated at −135 °C), and x_{water} is the weight fraction of water.

Previous works[30] show that polar solvents (water, alcohols, etc.) act as a plasticizer for some synthetic polymers such as polyamides. Nevertheless, the decrease of the glass transition temperature is less important in these cases because synthetic polymers cannot absorb a great quantity of water when compared to proteins.

In regime II, that is, for water weight fractions superior to 0.3, the glass transition T_g is independent of the weight fraction of water and remains equal to 0 °C, the melting temperature of crystallizable water.

The behavior of the noncrystallizable water of the macromolecular network is radically distinct from the behavior of the crystallizable water, characteristic of the water saturation of the studied protein. The melting of crystallizable water is also necessary to observe the transition from a glassy state to a rubbery state, and the glass transition temperature is superimposed to the melting phenomenon of water at 0 °C (see Figure 3). This effect, called "T_g regulation effect", is a simple consequence of the intersection of the Flory curve $T_g(x)$ with the solid $T_m(x)$ of water, as explained by Rault et al.[28,29] on the basis of DSC thermograms of polymer/water systems in cooling and heating experiments. Crystallizable water in the icelike form locks all the cooperative motions

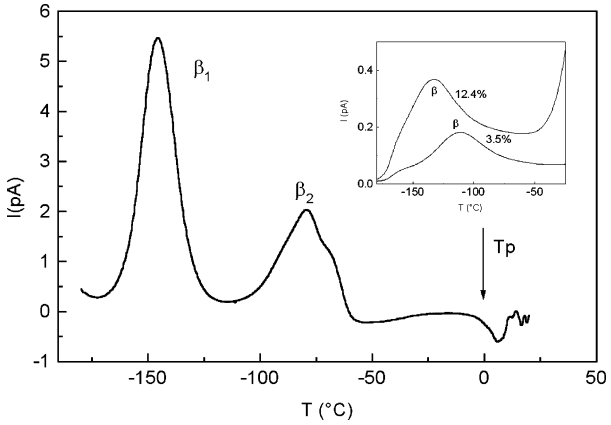

Figure 5. TSC spectrum of native elastin (noncrystallizable + crystallizable water), 50% hydrated. Inset: TSC spectrum of elastin with 12.4 and 3.5% hydration (from ref 1).

corresponding to a few nanometers, and the glass transition of the system, namely, the cooperative motions corresponding to some tens of nanometers, cannot occur before the melting of ice. So the lower temperature of the elastin−water glass transition is 0 °C.

We can estimate the critical water weight fraction x_c that delimits the two regimes; by identifying T_g in the Fox−Flory law to T_m, the melting temperature of water (approximatively 273.15 K for high concentrations of water, according to Raoult's law), we found that $x_c \approx 31\%$.

The heterogeneity of the hydration system allows us to bring to the forefront a structural heterogeneity in the elastin/water system, water acting as a probe of hydrophilic sites. For example, from the thermogram of the 40% hydrated elastin, the content of crystallizable water was estimated at 5% of the whole amount of water (by comparing the measure of melting enthalpy to the pure water melting enthalpy $\Delta H_m^{water} = 267.45\ J \cdot g^{-1}$). Because the mass sample was in this case equal to 11 mg, there was 4.4 mg of water, with 4.2 mg of noncrystallizable water occupying all the hydrophilic sites.

2. Dielectric Relaxations. This technique can be used to complement DSC to scan more localized motions than those associated with the glass transition and occurring at low temperature. We reported in a previous work[15] the TSC spectra of elastin for hydration levels between 0 and 12.4% (i.e., in the case of noncrystallizable water/elastin systems), obtained after a polarization at 0 °C.

Apart from the 0% hydrated sample (not shown here), all the spectra revealed a broad and well-defined peak (labeled β mode) located between −133 and −83 °C, depending on hydration: this evolution of the β mode is shown in the inset of Figure 5 for two levels of hydration). This β mode is widely affected by the noncrystallizable water content: it is shifted toward lower temperatures and magnified as the hydration level increases. This feature illustrates the plasticizing effect of water on the β relaxation, observed for the glass transition temperature.

According to literature data on a wide class of macromolecules such as polyamides,[30−32] polyamines, and proteins,[33,34] the great influence of water on the β mode leads us to associate it with localized relaxing polar sequences of the polypeptidic chain. The plasticizing effect at the nano-

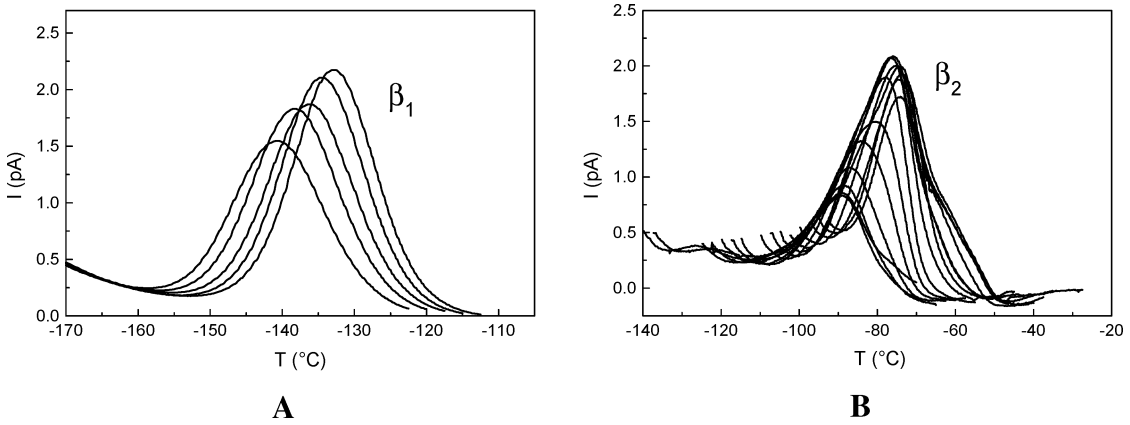

Figure 6. Experimental deconvolution of the TSC spectrum of 50% hydrated elastin by the FP method, for the $\beta 1$ mode (A) and for the β_2 mode (B).

metric scale is due to the replacement of protein/protein hydrogen bonds by protein/water hydrogen bonds that increase the mobility of the chains. Water molecules act as electrostatic screens between polar groups (mainly C═O and N—H), neutralizing the dipole/dipole interactions between polypeptidic units in folded proteins.

To follow the evolution of these localized relaxation modes when elastin fibers contain crystallizable water, we have reported in Figure 5 the TSC spectrum of native elastin, 50% hydrated, obtained after a polarization at 0 °C. A blocking electrode (Teflon electrode) was used in this case to suppress the parasite conduction, occurring when free water is heated above 0 °C.

Two main relaxation modes β_1 and β_2 are observed on this spectrum, located at around −145 and −80 °C, respectively. The β_2 mode is complex, possessing a shoulder on the high-temperature side. So we can infer the complexity of the dielectric answer at the nanometric scale from an increase of the number of interfaces in the hydrated elastin system due to free water.

Moreover, the intensity of the relaxation modes is much more important for the samples containing crystallizable water when compared to samples with noncrystallizable water only (there is a factor 10 between the intensities). This phenomenon can be explained by the increase of free volume when elastin is largely swelled by water; in this case, motions of larger amplitude (and so corresponding to larger dipoles) can occur in the system. We must also notice that the dipole value of water itself is important and contributes to the global increase of intensity.

To specify the molecular motions implied in the β_1 and β_2 modes, an experimental deconvolution of the TSC spectrum of hydrated elastin was done by the FP procedure. The polarization temperature was varied from −142.5 to −132.5 °C for the $\beta 1$ mode and from −95 to −62.5 °C for the $\beta 2$ mode, with $E_p = 400$ V/mm. This thermal cycling of the sample did not lead to physical aging of elastin because it performed at low temperature when compared to the glass transition of elastin. We plotted in Figure 6 the set of elementary spectra obtained from the β_1 and β_2 modes: each peak is well-fitted by a Debye peak and so can be associated with a single relaxation time $\tau(T)$. As we can see, the envelop of elementary spectra reproduces the global TSC spectra; a slight shift is observed between the global and elementary

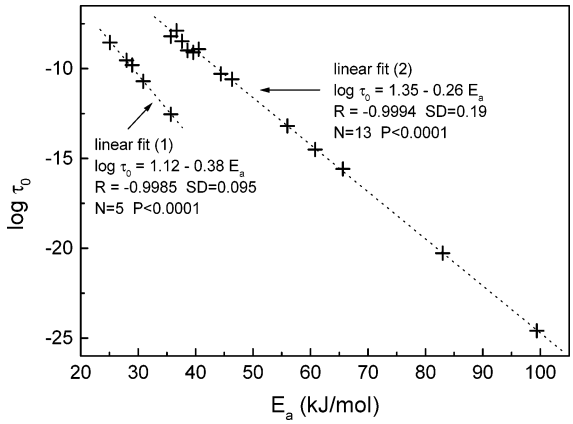

Figure 7. Variation of the preexponential factor versus the activation energy for the elementary relaxation times of a 50% hydrated elastin extracted from the FP method in the low-temperature range.

spectra for the $\beta 1$ mode as a result of the very low temperature of this mode; as a matter of fact, we cannot start the experimental deconvolution at the actual beginning of the mode (because of the limitation on T_0), and the first elementary spectra of the deconvolution are missing.

The FP method allows us to access the distribution of relaxation times of the low-temperature zone. By plotting the variation of $\tau(T)$ versus temperature, we noted that all the extracted relaxation times followed are well-fitted by an Arrhenius law:

$$\tau_i(T) = \tau_{0i} \exp(E_{ai}/RT)$$

where τ_i is the isolated relaxation time from the ith peak, T is the temperature, τ_{0i} an exponential factor, E_{ai} is the activation energy, and R is the ideal gas constant.

We reported in Figure 7 the variation of τ_0 versus E_a for all the isolated relaxation times: as we can see, a linear relationship is found between E_a and τ_0 for each zone of relaxation. This relationship can be expressed by the following equation:

$$\tau_0 = \tau_c \exp\left(-\frac{E_a}{RT_c}\right)$$

where τ_c and T_c are connected to the origin ordinate and to the slope of the straight line, respectively.

At the temperature T_c, all the related relaxation times would have the same value of τ_c, which is considered in the literature as a compensation phenomenon.[35,36] For the $\beta 1$ mode, there is not a large distribution in τ_0 and E_a; this mode is roughly a Debye peak. The value of the compensation temperature is $T_{c1} = -136$ °C, and the compensation time $\tau_{c1} = 13$ s. These results are very close from the previous works on the dielectric relaxation of pure ice I_h;[37] in this case, the global relaxation of ice obtained by dynamic dielectric spectroscopy obeys the following law:

$$\tau(T) = \tau_0 \exp\frac{E_a}{RT}$$

with $\tau_0 = 5.6 \times 10^{-12}$ s and $E_a = 30$ kJ/mol. We can observe that these results are very close from the mean values of the $\beta 1$ mode E_a and τ_0 distributions. Moreover, TSC studies of pure ice gave good evidence for the presence of a well-defined TSC peak at 131 K in the depolarization spectrum of ice;[38] these authors found the same ice peak by studying keratin−water at various states of hydration. The occurrence of a mode due to ice relaxation in this low-temperature range was also observed by dynamic mechanical experiments on collagen−water systems for high degrees of hydration;[39] all these results confirm that the $\beta 1$ mode observed for native elastin is undoubtedly attributed to the dielectric relaxation of ice *I*, which was previously attributed to the relaxation of frozen-in orientation polarization of water molecules in ice.

As for the $\beta 2$ mode, the E_a and τ_0 distributions are much more important (from 10^{-9} to 10^{-25} s and from 35 to 100 kJ/mol for τ_0 and E_a, respectively). The compensation parameters are $T_{c2} = -73$ °C and $\tau_{c2} = 22$ s. The activation energies correspond to the reorientation of larger dipoles than for the $\beta 1$ modes (the values of E_a in this case do not exceed 35 kJ/mol). Because a large compensation phenomenon is observed, we can suggest that the $\beta 2$ mode is a cooperative mode associated with the water/protein complex. Previous studies on different biopolymers/water or hydrated polymers with polar groups gave evidence of such a $\beta 2$ mode, and several explanations were made. For Leveque et al.,[40] this peak observed in keratin is due to the reorientation of bound or intermediate water molecules. In the case of collagen, this $\beta 2$ mode could correspond to the breaking and formation of hydrogen bonds between residues and structural water[39,41,42] or to precise entities of the collagen triple helix, like hydroxyproline strongly coupled to water.[43,44] In the case of swollen polymers such as polyamide and poly(vinyl acetate), which can form hydrogen bonds with water, like proteins, the β transition is usually due to the mobility of water molecules and chain ends.[32] As for hydrated elastin, the dielectric $\beta 2$ peak could be attributed to the relaxation of the complex elastin-bound water, which needs more energy to reorientate itself than free water and which must be a distributed relaxation, reflecting the distribution of water attachment sites along the polypeptidic chains. Previous dielectric works on hydrated proteins such as lyzozyme showed that bound water in this case behaves as a glassy system;[45] the large compensation observed for the $\beta 2$ mode, with values of τ_0 and E_a reaching maxima generally observed for the dielectric manifestation of glass transition in polymers, could indicate a similar glassy behavior of bound water in elastin. Finally, mechanical analysis of different elastin/polar solvent systems[34] evidenced such a relaxation mode, whose intensity and activation enthalpy increased with the size of the solvent (water, ethylene glycol, and triethylene glycol were tested), confirming our assumption.

Conclusion

This study shows that the combination of both thermal analysis and dielectric techniques is useful to characterize a biopolymer in the hydrated state; in the peculiar case of elastin, whose structure−function relationship is not totally elucidated, this work allows us to discuss the different models elaborated to explain the elasticity of elastin.

DSC gives information on the influence of water on the viscoeleactic properties of elastin, through the analysis of the glass transition temperature T_g.

We showed that water acts as a strong plasticizer for elastin, lowering T_g in a spectacular manner from 200 °C in the dehydrated state to room temperature for a 30% hydration level. However, the existence of a minimal glass transition temperature has been evidenced for high hydration levels (>40%), when elastin fibers contain crystallizable water. In this case, the motions of some tens of nanometers along the polypeptidic chains are blocked until the beginning of ice melting. So, noncrystallizable water, which can be roughly considered as bound water, linked to the polar atoms of the chain by hydrogen bonds,[14] plays a determinant role in increasing the mobility of elastin in the relaxed state. Moreover, these experimental results clearly illustrate the macroscopic amorphous character of elastin in the relaxed state. No transition associated with a long-range order is detected by DSC, which is in good agreement with Tamburro et al.'s model on labile, dynamic β turns in hydrophobic domains such as GXGGX sequences[1] and Li and Daggett's model,[14] which describes hydrophobic domains of elastin as compact amorphous structures.

TSC has allowed us to reach more localized motions (at the nanometric scale), undetectable by DSC, that occur at low temperature. In this case, the evolution of the local dipolar reorientations has been followed from the native to the dehydrated tissue, revealing an increasing complexity with coexisting elastin, noncrystallizable water, and crystallizable water. Despite the complexity of the observed phenomena, this preliminary dielectric study of elastin fibers in conditions close to physiological has been proved conclusive for studying a biological tissue under high hydration conditions. The dynamics of reorientation of crystallizable water, which can be roughly assimilated to free water, takes place at very low temperature and is weakly distributed in relaxation times because it concerns a slightly energetic motion, essentially noncooperative. The reorientation of the dipolar complex including non crystallizable water (assimilated to bound water) and dipolar groups of the elastin backbone is observed 70 °C higher because it is more energetic. Moreover, this mode is largely distributed, evidencing the large distribution of sites of attachment of water with the polypeptidic chain, which is in favor of a nonordered structure in the probed sequences.

The investigation of dipolar relaxations at higher temperature ($T > 0$ °C) that requires technical improvements is

now in progress and will complete this work. It will allow us to scan motions of larger amplitudes, such as the dielectric manifestation of the glass transition of elastin, and to check if more rigid or ordered sequences, like polyalanine regions, are detectable by dielectric techniques. Moreover, the methodology used in this study could be applied to other elastin polar solvents, like the elastin/dimethyl sulfoxide system (where elastin behaves as an ideal elastomer)[46] to obtain interesting additional data on the structural aspects of elastin swelled in polar solvents. These results should contribute to the understanding of the structure−function relationship of elastin.

References and Notes

(1) Debelle, L.; Tamburro, A. M. *Int. J. Biochem. Cell Biol*. **1999**, *31*, 261−272.
(2) Brown-Augsburger, P.; Tisdale, C.; Broekelmann, T.; Sloan, C.; Mecham, R. P. *J. Biol. Chem.* **1995**, *270*, 17778−17783.
(3) Brown-Augsburger, P.; Tisdale, C.; Broekelmann, T.; Rosenbloom, J.; Mecham, R. P. *Biochem. J.* **1996**, *318*, 149−155.
(4) Martino, M.; Perri, T.; Tamburro, A. M. *Biomacromolecules* **2002**, *3*, 297−304.
(5) Gotte, L. *Front. Matrix Biol.* **1980**, *8*, 33−53.
(6) Hoeve, C. A. J.; Flory, P. J. *Biopolymers* **1974**, *13*, 677−686.
(7) Lillie, M. A.; Gosline, J. M. *Biopolymers* **1990**, *29*, 1147−1160.
(8) Foster, J. A.; Rubin, L.; Kagan, H. M.; Franzblau, C.; Bruenger, E.; Sandberg, L. B. *J. Biol. Chem.* **1974**, *249*, 6191−6196.
(9) Urry, D. W. *Ultrastruct. Pathol.* **1983**, *4*, 227−251.
(10) Urry, D. W. *J. Protein Chem.* **1984**, *3*, 403−436.
(11) Urry, D. W. *Int. J. Quantum Chem., Quantum Biol. Symp*. **1987**, *14*, 261−280.
(12) Gray, W. R.; Sandberg, L. B.; Foster, J. A. *Nature* **1973**, *246*, 461−466.
(13) Urry, D. W.; Hugel, T.; Seitz, M.; Gaub, H. E.; Sheiba, L.; Dea, J.; Xu, J.; Parker, T. *Philos. Trans. Royal. Soc. London, Ser. B* **2002**, *357*, 169−184.
(14) Li, B.; Daggett, V. *J. Muscle Res. Cell Motil.* **2002**, *23*, 561−573.
(15) Samouillan, V.; Dandurand, J.; Lacabanne, C.; Hornebeck, W. *Biomacromolecules* **2002**, *3*, 531−537.
(16) Lansing, A. I.; Rosenthel, T. B.; Alex, M.; Dempsey, E. W. *Anat. Rec*. **1952**, *114*, 555−570.
(17) Reading, M.; Elliott, D.; Hill, V. L. *J. Therm. Anal*. **1993**, *40*, 949−955.
(18) Teyssedre, G.; Mezghani, S.; Bernes, A.; Lacabanne, C. Thermally stimulated currents of polymers. In *Dielectric spectroscopy of polymeric materials. Fundamental and applications*; Runt, J. P., Fitzgerald, J. J., Eds.; American Chemical Society: Washinton, DC, 1997; pp 227−255.
(19) Bucci, C.; Fieshi, R.; Guidi, G. *Phys. Rev.* **1966**, *148*, 816−833.
(20) McCrum, N. G.; Read, G.; Williams, B. E. *Anelastic and dielectric effects in polymeric solids*; John Wiley: New York, 1967.
(21) Struik, L. C. E. *Physical aging in amorphous polymers and other materials*; Elsevier: Amsterdam, 1978.
(22) Villani, V.; Tamburro, A. M. *J. Biomol. Struct. Dyn.* **1995**, *12*, 1173−1202.
(23) Villani, V.; Tamburro, A. M.; Zaldivar Comenges, J. *J. Chem. Soc., Perkin Trans.* **2000**, *2*, 2177−2184.
(24) Tamburro, A. M. In *Elastin 2002*; Tamburro, A. M., Pepe, A., Eds.; Editric Ermes: Potenza, Italy, 2002; pp 3−14.
(25) André, C. *DEA report*; Paul Sabatier University: Toulouse, France, 2001.
(26) Froix, M. F.; Nelson, R. *Macromolecules* **1975**, *8*, 726−730.
(27) Cecorrulli, G.; Scandola, M.; Pezzin, G. *Biopolymers* **1977**, *16*, 1505−1512.
(28) Rault, J.; Lucas, A.; Neffati, R.; Monleon Pradas, M. *Macromolecules* **1997**, *30*, 7866−7873.
(29) Rault, J.; Gref, R.; Ping, Z. H.; Nguyen, Q. T.; Néel, J. *Polymer* **1995**, *36*, 1655−1661.
(30) Jaffe, M.; Menczel, J. D.; Bessey, W. E. In *Thermal Characterization of Polymeric Materials*; Turi, E. A., Ed.; Academic Press: New York, 1997; pp 1767−1954.
(31) Pathmanathan, K.; Cavaillé, J. Y.; Johari, G. P. *J. Polym. Sci., Part B: Polym. Phys.* **1992**, *30*, 341−348.
(32) Le Huy, H. M.; Rault, J. *Polymer* **1994**, *35*, 136−139.
(33) Bone, S.; Pethig, R. *J. Mol. Biol*. **1985**, *181*, 323−326.
(34) Andrady, A. L.; Mark, J. E. *Polym. Bull*. **1991**, *27*, 227−234.
(35) Samouillan, V.; Lamure, A.; Maurel, E.; Lacabanne, C.; Hornebeck, W. *Biopolymers* **2001**, *58*, 175−185.
(36) Lavergne, C.; Lacabanne, C. *IEEE Elec. Insul. Mag*. **1993**, *9*, 5−21.
(37) Johari, G. P.; Whalley, E. *J. Chem. Phys.* **1981**, *75*, 1333−1340.
(38) Leveque, J. L.; Garson, J. C.; Pissis, P.; Boudouris, G. *Biopolymers* **1981**, *20*, 2649−2656.
(39) Nomura, S.; Hiltner, A.; Lando, J. B.; Baer, E. *Biopolymers* **1977**, *16*, 231−246.
(40) Leveque, J. L.; Garson, J. C.; Boudouris, G. *Biopolymers* **1977**, *16*, 1725−1733.
(41) Chien, J. C. W.; Chang, E. P. *Biopolymers* **1972**, *11*, 2015−2031.
(42) Nguyen, A. L.; Vu, B. T.; Wilkes, G. L. *Biopolymers* **1974**, *13*, 1023−1037.
(43) Yau, B. J.; Woodward, A. E.; Gilbert, S. G. *J. Appl. Phys.* **1978**, *49*, 5068−5073.
(44) Maeda, H.; Fukada, E. *Biopolymers* **1982**, *21*, 2055−2069.
(45) Peyrard, M. *Phys. Rev. E*. **2001**, *64*, 11109-1−11109-5.
(46) Mistrali, F.; Volpin, D.; Garibaldo, G. B.; Ciferri, A. *J. Phys. Chem*. **1971**, *75*, 142−149.

BM034436T